Microelectronic Engineering 126 (2014) 179–183

Contents lists available at ScienceDirect

Microelectronic Engineering

journal homepage: www.elsevier.com/locate/mee

SiC pinpin photonic filters for linking the visible spectrum to the telecom gap

M. Vieira [a,b,c,*], M.A. Vieira [a,b], P. Louro [a,b], A. Fantoni [a,b], V. Silva [a]

[a] Electronics Telecommunication and Computer Dept. ISEL, R. Conselheiro Emídio Navarro, 1949-014 Lisboa, Portugal
[b] CTS-UNINOVA, Quinta da Torre, Monte da Caparica, 2829-516 Caparica, Portugal
[c] DEE-FCT-UNL, Quinta da Torre, Monte da Caparica, 2829-516 Caparica, Portugal

ARTICLE INFO

Article history:
Received 14 October 2013
Received in revised form 5 June 2014
Accepted 20 June 2014
Available online 21 July 2014

Keywords:
Optoelectronic devices
Tandem heterostuctures
WDM devices
Telecommunications

ABSTRACT

Expanding far beyond traditional applications at telecommunications wavelengths, the SiC photonic devices has recently proven its merits for working with visible range optical signals. Reconfigurable wavelength selectors are essential sub-systems for implementing reconfigurable WDM networks and optical signal processing. Visible range to telecom band spectral translation in SiC/Si can be accomplished using wavelength selector under appropriated optical bias, acting as reconfigurable active filters. In this paper we present a monolithically integrated wavelength selector based on a multilayer SiC/Si integrated optical filters that requires optical switches to select wavelengths. The selector filter is realized by using double pin/pin a-SiC:H photodetector with front and back biased optical gating elements. Red, green, blue and violet communication channels are transmitted together, each one with a specific bit sequence. The combined optical signal is analyzed by reading out the generated photocurrent, under different background wavelengths applied either from the front or the back side. The backgrounds acts as channel selectors that selects one or more channels by splitting portions of the input multi-channel optical signals across the front and back photodiodes. The transfer characteristics effects due to changes in steady state light, irradiation side and frequency are presented. The relationship between the optical inputs and the digital output levels is established.

1. Introduction

Multi-disciplinary technologies for telecommunication systems have evolved from material systems for LEDs and lasers sources to optical fiber technology and photo detection materials. Newly developed technologies, for infrared telecommunication systems, allowed increase of capacity, distance and functionality. Far beyond traditional applications in optical interconnects at telecommunications wavelengths, the SiC nanophotonic integrated circuit platform has recently proven its merits for working with visible range optical signals [1,2].

In order to enhance the transmission capacity and the application flexibility of optical communication and sensor systems, associated efforts have to be considered, namely: Wavelength Division Multiplexing (WDM) based on amorphous technology when different optical signals are encoded in the same optical transmission path; the IP-based multimedia services architecture to provide transparent communication over different networks [3], switching and control with the design of new reconfigurable logic active filter gates by "bridging the gaps" and combining the optical filters properties [4,5].

The SiC tuneable background filters are used to perform several filtering processes and then different signal processing functions: amplification, switching, and wavelength conversion [1]. In this paper the SiC tunable background filters form the bridge between the infrared and visible windows. The device can be used as a bistable optical gate acting either as a short- or a long- pass band filter or as a band-stop filter, depending on the wavelength of the external background. In consequence, bridging the visible spectrum to telecom gap offers the opportunity to provide alternative and additional low cost services to improve operative production processes in office, home and automotive networks.

Some directions for further research will be suggested. These include also improvements for integrated optics technology, optical receiver design, visible range-like techniques, relational algorithms, routing and wavelength conversion.

* Corresponding author at: Electronics Telecommunication and Computer Dept. ISEL, R. Conselheiro Emídio Navarro, 1949-014 Lisboa, Portugal. Tel.: +351 21 8317290; fax: +351 21 8317114.
E-mail address: mv@isel.ipl.pt (M. Vieira).

http://dx.doi.org/10.1016/j.mee.2014.06.033
0167-9317/

2. Device design, characterization and operation

The wavelength selector filter is realized by using double pin/pin a-SiC:H photodetector with front and back biased optical transparent conductive oxide (TCO) gating elements as depicted in Fig. 1. The sensor is 1 cm^2 of two stacked p-i-n structures (p(a-SiC:H)-i′(a-SiC:H)-n(a-SiC:H)-p(a-SiC:H)-i(a-Si:H)-n(a-Si:H)) with low conductivity doped layers deposited by PECVD sandwiched between two transparent contacts ITO (indium tin oxide) produced by thermal evaporation one at each end. The deposition conditions and optoelectronic characterization were described elsewhere [1]. The thicknesses and optical gap of the front i′- (200 nm; 2.1 eV) and back i- (1000 nm; 1.8 eV) layers are optimized for light absorption in the blue and red ranges, respectively [6]. In Fig. 1 the arrows indicate the absorption depths of the different wavelength channels during operation and λ_V, λ_B, λ_G, λ_R the digital light signals.

Red, green, blue and violet pulsed communication channels ($\lambda_{R,G,B,V}$; input channels) are transmitted together, each one with a specific bit sequence. The combined optical signal (multiplexed signal) is analyzed by reading out the generated photocurrent under negative applied voltage (−8V), without and with violet background (λ = 400 nm) applied either from the device front or back sides. The device operates within the visible range using as input color channels (data) the wave square modulated light (external regulation of frequency and intensity) supplied by a red (R: 626 nm; 25 W/cm^2), a green (G: 524 nm; 46 W/cm^2), a blue (B: 470 nm; 40 W/cm^2) and a violet (V: 150 W/cm^2) LED's. The steady state violet irradiation (optical bias) was superimposed using a LED (400 nm; 2800 W/cm^2).

The spectral sensitivity under violet background and without it was tested through spectral response measurements applied either from the front or back side of the device (Fig. 2). Using a monochromator with 1 mm slits and a chopper frequency of 3500 Hz the sensor was continually biased with −8V and measurements made from 400 to 800 nm in 10 nm steps in three conditions: dark, front, back. In the dark condition, the sensor is only subjected to the monochromator's light source. These measurements are considered as a reference. The back or front conditions refer to a steady illumination of the back or front side of the sensor. This background illumination was made with a 400 nm LED.

In Fig. 2a the optical bias was applied from the front side and in Fig. 2b from the back side. For comparison the normalized spectral photocurrent for the front, p-i′-n, and the back, p-i-n, photodiodes (dash lines) are superimposed.

Data shows that the front and back diodes, separately, presents the typical responses of single p-i-n cells with intrinsic layers based on a-SiC:H or a-Si:H materials, respectively. The front diode

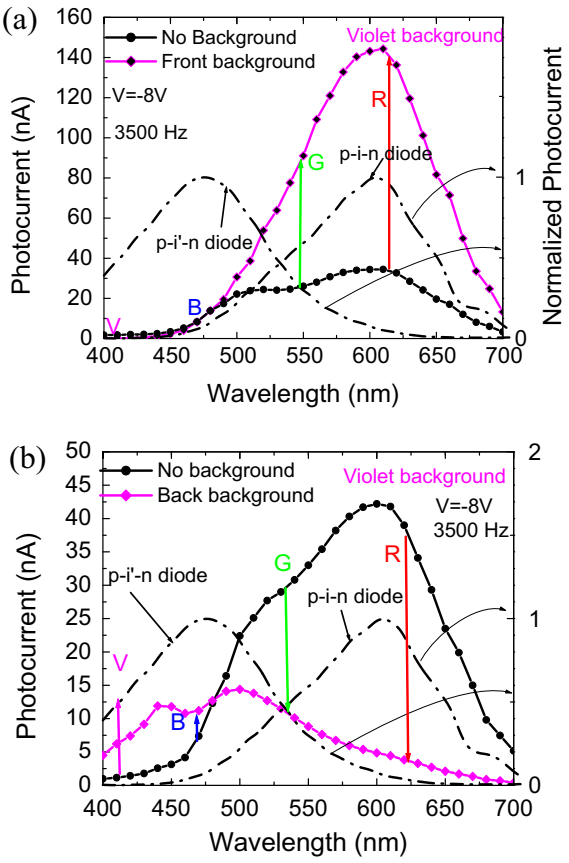

Fig. 2. Photocurrent without and with front (a) and back (b) violet background (symbols). The normalized photocurrent of the individual photodiodes is superimposed (dash lines). (For interpretation of the references to color in this figure legend, the reader is referred to the web version of this article.)

cuts the wavelengths higher than 550 nm while the back one rejects the ones lower than 500 nm. The overall device presents an enlarged sensitivity when compared with the individual ones.

Under front irradiation the sensitivity is much higher than under back irradiation. Under front irradiation the violet background amplifies the spectral sensitivity mainly in the long wavelength range (>550 nm) while back irradiation strongly quenches this and enhances the short wavelength range (see arrows in both figures). Thus, back irradiation, tunes the front diode while front irradiation selects the back one.

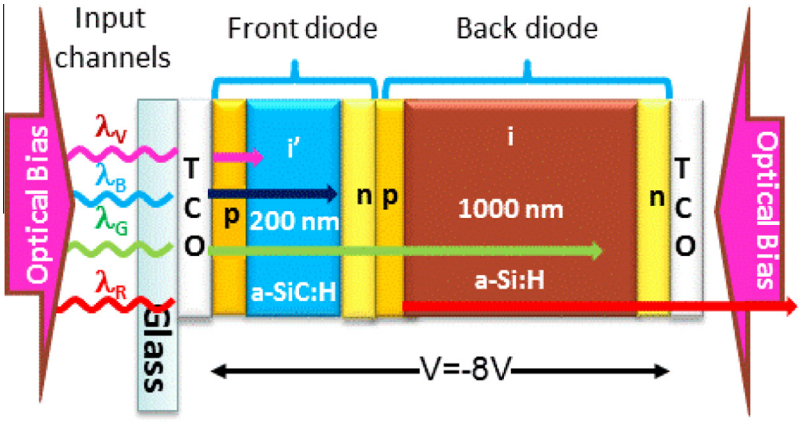

Fig. 1. (a) Device configuration and operation. The wavelength arrows indicate the absorption depths during operation and λ_V, λ_B, λ_G, λ_R the digital light signals.

3. Optical bias amplification

To analyze the device under information-modulated wave and uniform irradiation, four monochromatic pulsed lights, separately (red, green, blue and violet input channels; R, G, B, V) illuminated the device at 12,000 bps. Steady state violet optical bias was superimposed separately from the front (Fig. 3a) and the back (Fig. 3b) sides and the photocurrent generated measured at −8 V. In both figures the signals, without applied optical bias, are shown. The ratio between the photocurrents with and without background (amplification factor) for the four individual channels (α_{Rfront}, α_{Gfront}, α_{Bfront}, α_{Vfront}) are also displayed. The arrows and their direction guide the eyes into the quenching or enhancement due to the optical bias.

Results show that when steady state irradiation is imposed the output photocurrent due to the input signals exhibits a nonlinear dependence on the wavelength. Under front irradiation, the light-to-dark sensitivity is enhanced mainly in the long-medium wavelength ranges. Violet radiation is absorbed at the top of the front diode, increasing the electric field at the least absorbing cell [7], the back diode, where the red and part of the green channels generate optical carriers. So, red and green collection are strongly enhanced ($\alpha_{Rfront} = 4.7$, $\alpha_{Gfront} = 2.4$), the blue lightly increases ($\alpha_{Bfront} = 1.3$) and the violet one stays near its dark value ($\alpha_{vfront} = 1.0$). Under back irradiation, the small absorption depth of the violet photons in the back diode enhances the electric field at the front diode and so, the red and green collections are reduced ($\alpha_{Rback} = 0.5$, $\alpha_{Gback} = 0.6$). The violet and the blue channels are absorbed across the front diode resulting in an increase collection for the blue ($\alpha_{Bback} = 1.5$) and enormous increase for the violet ($\alpha_{Vback} = 11.0$) since its absorption occurs near the front p-i′ interface where the electric field suffers the larger increase.

4. Data selector

In Fig. 4a the combined signal (multiplexed signal) is displayed with front and back violet background. In Fig. 4b the difference between the multiplexed signals under front and back irradiation, the so called wavelength-generation rate, is depicted. On the top the signals used to drive the input channels are shown to guide the eyes into the ON/OFF states of each input. In Fig. 4b, for comparison the signal under front irradiation is added.

Under front irradiation, data shows that the encoded signal (output) presents sixteen ordered levels (2^4 inputs, dotted lines) each one related with an RGBV bit sequence (right side of Fig. 4a). The signal magnitude is balanced by the channel amplification factor (Fig. 3a, $\alpha_{RGBV,front}$) of each input. Depending on the presence or lack of an input signal, respectively 1 or 0 in a binary code, and on its amplification factor, the levels can be grouped into subgroups. The highest amplification of the red channel allows the division of the 16 inputs into two groups of 8 entries each: the upper 8 ascribed to the presence of the red channel (R = 1) and the lower 8 to its absence (R = 0). The green channel presents a medium amplification, so, the four (2^2) highest levels, of each group of 8, are ascribed to the presence of the green channel (G = 1) and the four lower ones to its lack (G = 0). The blue channel is slightly amplified, so, in each group of 4 entries, two groups (2^1) can be found: the two higher levels correspond to the presence of the blue channel (B = 1) and the two lowers to its absence (B = 0). Finally, each group of 2 entries have two sublevels, the higher

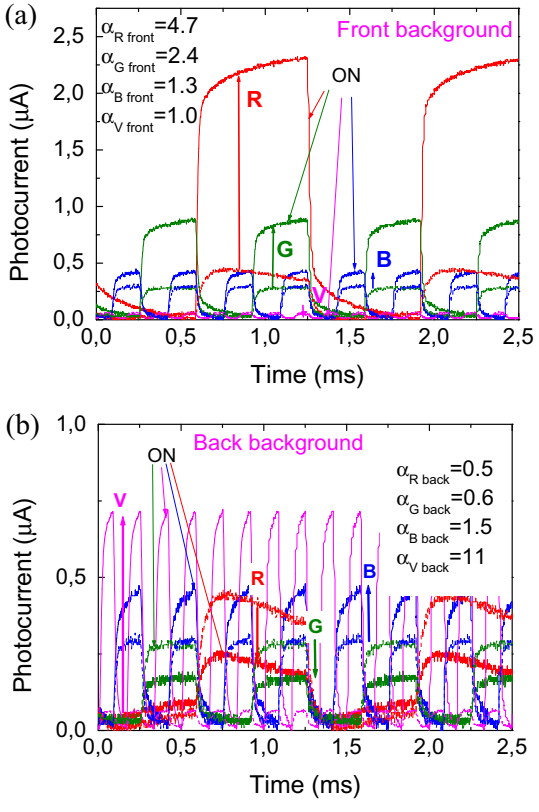

Fig. 3. Red (R), green (G) and blue (B) and violet (V) input channels, at −8V, without and under violet steady state optical bias (ON) applied from the front (a) and from the back (b) sides. The individual gains of each channel are displayed as inserts. The arrows and their direction guide the eyes into the quenching or enhancement due to the optical bias. (For interpretation of the references to color in this figure legend, the reader is referred to the web version of this article.)

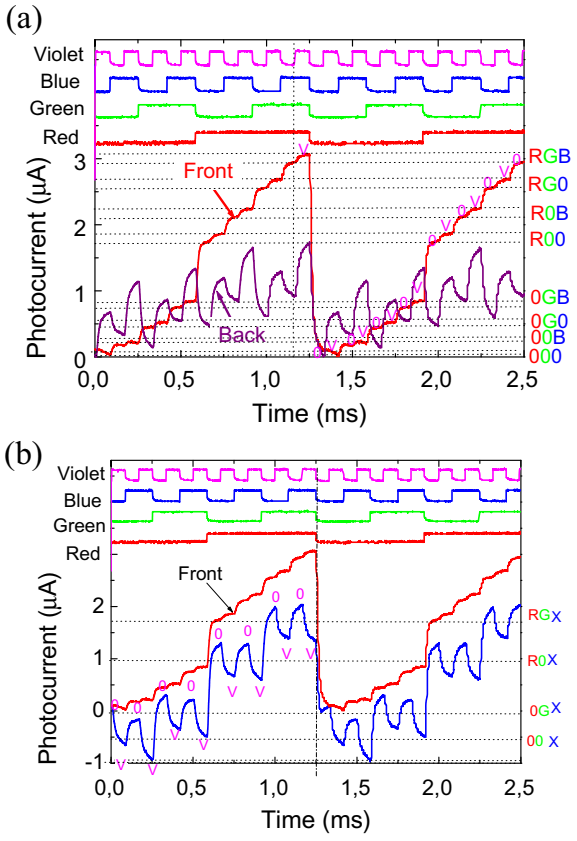

Fig. 4. (a) Multiplexed output signal under front and back violet irradiation. (b) Wavelength difference generation. On the top the signal to drive the input channels guide the eyes. The correspondent binary codes at the different photocurrent levels were added as inserts. (For interpretation of the references to color in this figure legend, the reader is referred to the web version of this article.)

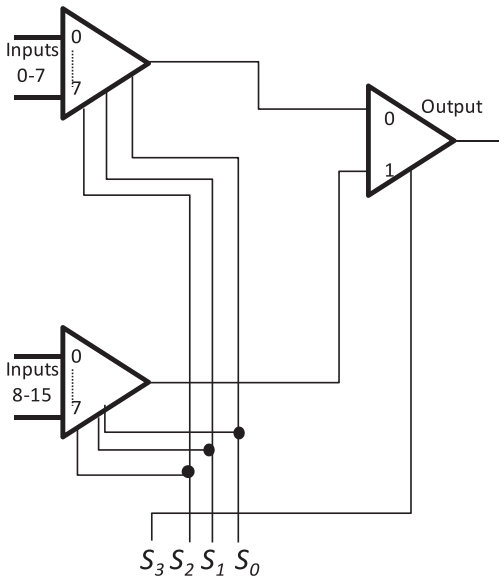

Fig. 5. Schematic of a pin/pin a-SiC:H 16-element table look-up. The selection index is a 4-bit binary S_3, S_2, S_1, S_0 where Sn means the color channel with n proportional to the amplification factor.

where the violet channels is ON (V = 1) and the lower where it is missing (V = 0). The selection index for this 16-element look-up table is a 4-bit binary R, G, B, V code of the form S_3, S_2, S_1, S_0 where Sn means the color channel (Fig. 4a) with n proportional to the amplification factor (Fig. 3a). So, the multiplexer select code, under front irradiation, represents an address (RGBV), or index, into the ordered inputs.

Under back irradiation the amplification factors change in an opposite way (Fig. 3b), the violet and blue channels are enhanced and the green and red reduced. The high amplification of the violet channel allows the division of the 16 inputs into two main groups of 8 entries each. The uppers 8 ascribed to the presence of the violet channel (V = 1) and the lower 8 to its absence (V = 0) acting as a 8-to-1 multiplexer. In each group the 4 higher levels have the blue channel ON and the others OFF (4-to-1 multiplexer). The upper level has both red and the green channels ON and the lower both OFF, in the other two middle entries only one of these channels is present. So, the 4-bit binary multiplexer select code represents a VBGR address into the ordered input. We may view the 16-element look-up table as consisting of two look-ups, one to select the proper group of 8, and pick the red under front irradiation (S_3 = R) or the violet under back background (S_3 = V). Each group of 8 inputs requires 3 bits for picking the proper group of 8 and for specifying an input (S_2, S_1, S_0). In Fig. 5 the schematic of the pin/pin a-SiC:H 16-element table look-up is displayed. Here, if S_3 = R then the S_2 = G, S_1 = B and S_0 = V; if S_3 = V the 4-bit binary code will be BGR.

5. Data router

Whereas the multiplexer is a data selector, the demultiplexer is a data distributor or data router. Just as the multiplexer has a binary code (RGBV) for the selection of an input, the demultiplexer has a similar code for selecting a particular output. In the pi'n/pin device the side of the background is the routing control for the data

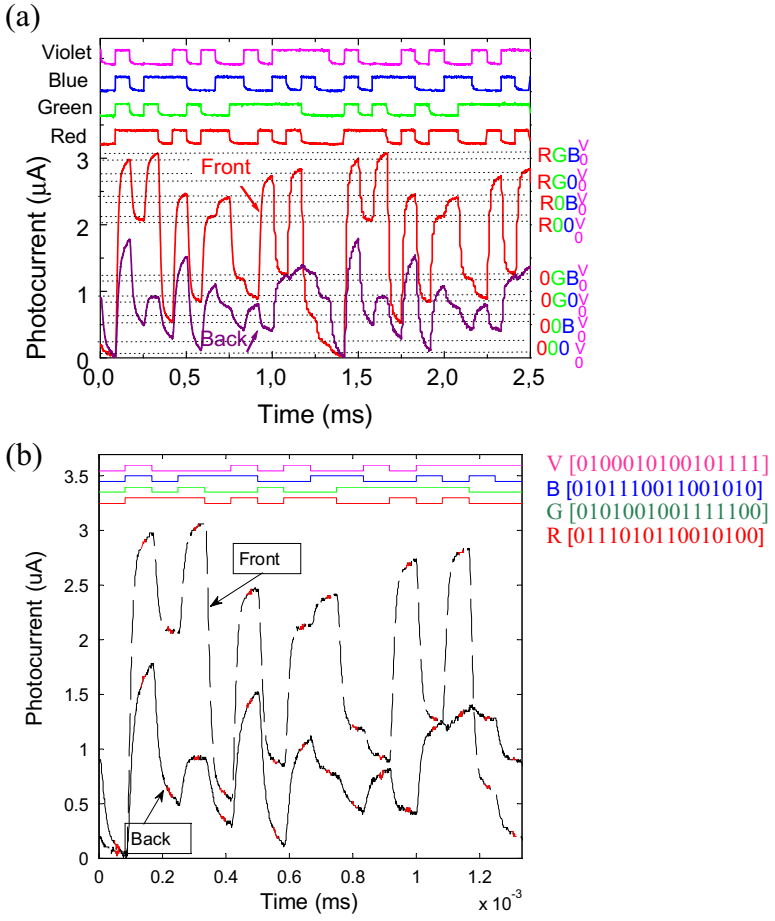

Fig. 6. MUX signal under front and back irradiation. On the top (a) signals used to drive the LED's. (b) DEMUX signals and decoded RGBV binary bit sequences.

source. The front and back background acts as selector to select one of the four incoming channels by splitting portions of the input multi-channel optical signal across the front and back photodiodes (Fig 2, see arrows). This duality of functions is characteristic of decoders and demultiplexers.

Under front background the red channel is decoded due to its higher amplification while under back violet irradiation the violet channel is selected (Fig. 4a). To help to decode the green and blue channels, in Fig. 4b the difference between the multiplex signal under front and back violet irradiation is displayed. This difference wavelength generation is a consequence of nonlinear interaction of the device with the front or back backgrounds and the optical channels generation. It weights the red versus violet content of the measured signal, so, it enhances the effect of the routing control and offers a transparent wavelength conversion.

The presence of the red channel pushes the difference up and the violet channel pushes it down (right side of Fig. 4b). The blue channel does not affect the difference. So, after decoding the red and the violet transmitted information and comparing with difference wavelength generation levels in the same time slots, the green and blue signals can be immediately decoded. We have used this simple algorithm to perform 1-to-16 demultiplexer (DEMUX) function and to decode the multiplex signals.

As proof of concept the decoding algorithm was implemented in *Matlab* [8] and tested using different binary sequences. In Fig. 6a a random MUX signal under front and back irradiation is displayed and in Fig. 6b the decoding results are shown. On the top of both figures the signals to drive the LED's and the DEMUX signals obtained as well as the binary bit sequences are respectively displayed. A good agreement between the signals used to drive the LED's and the decoded sequences is achieved. In all sequences tested the RGBV signals were correctly decoded.

The DEMUX sends the input logic signal to one of its sixteen outputs, according to the optoelectronic DEMUX algorithm. So, by means of optical control applied to the front or back diodes, the photonic function is modified, respectively from a long- pass filter to pick the red channel to a short-pass filter to select the violet channel, giving a step reconfiguration of the device. The green and blue channels are selected by combining both active long- and short-pass filters into a band-pass filter. In practice, the decoding applications far outnumber those of demultiplexing. Multilayer SiC/Si optical technology can provide a smart solution to communication problem by providing a possibility of optical bypass for the transit traffic by dropping the fractional traffic that is needed at a particular point.

6. Conclusions

A monolithically integrated wavelength selector based on SiC multilayer photonics active filters is analyzed. Tailoring the filter wavelength was achieved by changing the violet background side. Results show that the pin/pi'n multilayered structure becomes reconfigurable under front and back irradiation, acting either as data selector or data router. It performs WDM optoelectronic logic functions providing photonic functions such as signal amplification, filtering and switching.

A 16-element look-up table was presented. The selection index is a 4-bit binary RGBV code under front irradiation and VBGR under back light. An algorithm to decode the four input channels is presented.

Using visible light for data transmission opens a broad spectrum of applications, such as photonic circuits for the purpose of chip-level communications and location estimation. Increases in power efficiency per bit of data is projected to be achieved by replacing electrical interconnects with their optical counterparts in the near future. Future work has to be done in order to increase the modulation frequency of the light.

Acknowledgments

This work was supported by FCT (CTS multi annual funding) through the PIDDAC Program funds and PTDC/EEA-ELC/111854/2009 and PTDC/EEA-ELC/120539/2010.

References

[1] M. Vieira, P. Louro, M. Fernandes, M.A. Vieira, A. Fantoni, J. Costa, Advances in Photodiodes, InTech, 2011. pp. 403–425 (Chapter 19).
[2] M.A. Vieira, M. Vieira, J. Costa, P. Louro, M. Fernandes, A. Fantoni, Sens. Transducers J. (2010) 96–120 (Special Issue).
[3] Z. Zhongwen, J. Multimedia Ubiquitous Eng. 3 (4) (2008) 17–24.
[4] P.P. Yupapin, P. Chunpang, Int. J. Light Electron. Opt. 120 (18) (2009) 976–979.
[5] S. Ibrahim, L.W. Luo, S.S. Djordjevic, C.B. Poitras, I. Zhou, N.K. Fontaine, B. Guan, Z. Ding, K. Okamoto, M. Lipson, S.J.B. Yoo, Paper OWJ5, Optical Fiber Communications Conference, OSA/OFC/NFOEC, San Diego, 21 Mar 2010.
[6] M.A. Vieira, P. Louro, M. Vieira, A. Fantoni, A. Steiger-Garção, IEEE Sens. J. 12 (6) (2012) 1755–1762.
[7] M. Vieira, A. Fantoni, P. Louro, M. Fernandes, R. Schwarz, G. Lavareda, C.N. Carvalho, Vacuum 82 (12) (2008) 1512–1516.
[8] M.A. Vieira, M. Vieira, J. Costa, P. Louro, M. Fernandes, A. Fantoni, Sens. Transducers J. 10 (2011) 96–120 (Special Issue).